

Review

Recent Progress of Ferroelectric-Gate Field-Effect Transistors and Applications to Nonvolatile Logic and FeNAND Flash Memory

Shigeki Sakai * and Mitsue Takahashi

National Institute of Advanced Industrial Science and Technology / Central 2, 1-1-1 Umezono, Tsukuba, Ibaraki 305-8568, Japan; E-Mail: mitsue-takahashi@aist.go.jp

* Author to whom correspondence should be addressed; E-Mail: shigeki.sakai@aist.go.jp; Tel.: +81-29-861-5468; Fax: +81-29-861-5476.

Received: 18 October 2010; in revised form: 12 November 2010 / Accepted: 16 November 2010 / Published: 18 November 2010

Abstract: We have investigated ferroelectric-gate field-effect transistors (FeFETs) with Pt/SrBi₂Ta₂O₉/(HfO₂)_x(Al₂O₃)_{1-x} (Hf-Al-O) and Pt/SrBi₂Ta₂O₉/HfO₂ gate stacks. The fabricated FeFETs have excellent data retention characteristics: The drain current ratio between the on- and off-states of a FeFET was more than 2×10^6 after 12 days, and the decreasing rate of this ratio was so small that the extrapolated drain current ratio after 10 years is larger than 1×10^5 . A fabricated self-aligned gate Pt/SrBi₂Ta₂O₉/Hf-Al-O/Si FET revealed a sufficiently large drain current ratio of 2.4×10^5 after 33.5 day, which is 6.5×10^4 after 10 years by extrapolation. The developed FeFETs also revealed stable retention characteristics at an elevated temperature up to 120 °C and had small transistor threshold voltage (V_{th}) distribution. The V_{th} can be adjusted by controlling channel impurity densities for both *n*-channel and *p*-channel FeFETs. These performances are now suitable to integrated circuit application with nonvolatile functions. Fundamental properties for the applications to ferroelectric-CMOS nonvolatile logic-circuits and to ferroelectric-NAND flash memories are demonstrated.

Keywords: FeFET; semiconductor memory; nonvolatile memory; nonvolatile logic

1. Introduction

As a nonvolatile memory, ferroelectric-gate field-effect-transistors (FeFETs) have many advantages in high-density integration, low power dissipation, non-destructive readout operation, and good scalability [1]. A variety of FeFETs had been investigated over the past decades [2-10]. However, despite much effort by a lot of research groups, data retention time of the FeFETs has been short. In order to explain the cause of this short data retention, the effects of depolarization field [11] and unsaturated polarizations [12] in ferroelectric layers have been discussed.

A promising gate-material combination of metal/ferroelectric/insulator/semiconductor (MFIS) and a good process for FeFETs having long data retention were found by the author (S.S.) in 2002 [13-18]. Since then, FeFETs became a real candidate for practical nonvolatile memories. We have continuously studied not only further technological development of FeFETs but also FeFET applications to integrated circuits. We are now investigating two kinds of applications of the FeFETs, which are FeCMOS nonvolatile logic circuits and FeNAND flash memories. Note that FeFETs based on different materials and on different types have been investigated during the last decade, which are listed only partially in [19-26].

In this paper, we will first describe our FeFET development, and second, we will show recent results of the FeFET applications to FeCMOS and FeNAND flash memories.

2. Progress of Ferroelectric-Gate Field-Effect-Transistors

The promising material combination of the MFIS gate stack discovered in 2002 was Pt/SrBi₂Ta₂O₉/(HfO₂)_x(Al₂O₃)_{1-x}/Si. Hereafter, SrBi₂Ta₂O₉ and (HfO₂)_x(Al₂O₃)_{1-x} are abbreviated as SBT and Hf-Al-O, respectively. A schematic cross section is shown in Figure 1. The I_d vs. gate voltage (V_g) characteristic for an n -channel MFIS FET ($x = 0.75$) is shown in Figure 2 [15]. When the applied V_g was varied from -6.0 V to $+6.0$ V, a hysteresis loop with a wide memory window of 1.6 V and a large $I_{d,on}/I_{d,off}$ ratio over 10^7 at $V_g = 1.7$ V was obtained due to the ferroelectricity. The I_d increase at negative V_g in Figure 2 is not due to a gate leakage current, but due to a current between the p -type substrate and the n^+ -drain. This I_d increase was closely correlated to the overlap length of the drain and gate. When this overlap length was shortened, the drain current increase at the negative gate voltage was lowered. Thus, the increased current at the negative gate voltages is a gate-induced leakage current (GIDL) between the drain bulk (n^+) and the drain-surface inversion (p) layer under the gate area [15].

Figure 3 shows I_d data retention characteristics of the MFIS FET [13-18]. During the $I_{d,on}$ retention measurement, V_g was kept at a bias gate voltage $V_{keep} = 1.7$ V after $V_g = +6.0$ V was applied to polarize the ferroelectric SBT. For the $I_{d,off}$ retention measurement, V_g was kept at the same bias gate voltage, $V_{keep} = 1.7$ V, after $V_g = -6.0$ V was applied. Both the $I_{d,on}$ and $I_{d,off}$ retention characteristics were measured up to 10^6 s (12 days). The $I_{d,on}/I_{d,off}$ ratio was about 10^7 immediately after data writing and still larger than 10^6 after 12 days. A plot of the memory window vs. the applied V_g amplitude or scan voltage is shown in the inset of Figure 2. The inset indicates that the ferroelectric polarization is not saturated yet at a scan voltage of 8.0 V. This concludes that the usage of saturated polarization is not a necessary condition to get FeFETs with long retention. The fact that a FeFET with long retention

was achieved means that nonvolatile FeFETs can work even under the presence of the depolarization field in the MFIS gate stack.

Figure 1. Schematic cross section of a fabricated FeFET. Gate, ferroelectric and insulator are made of Pt, SBT and Hf-Al-O, respectively. Reprinted from [17] with permission of the Japan Society of Applied Physics.

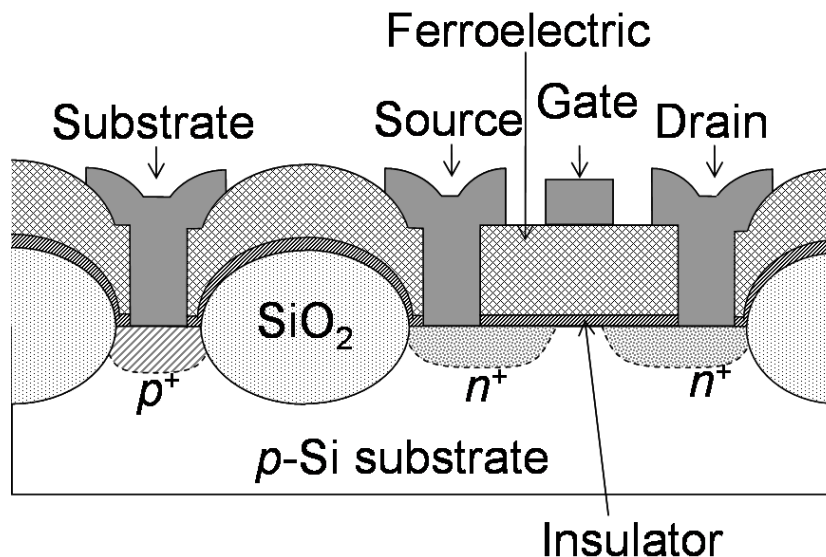


Figure 2. Drain current-gate voltage curves of an *n*-channel Pt/SBT/Hf-Al-O/Si FeFET at $V_g = \pm 6.0$ V. The inset was made by measuring the curves at $V_g = \pm 4.0, \pm 5.0, \pm 6.0, \pm 7.0$ and ± 8.0 V. Scan voltage is each gate-voltage amplitude applied to the FeFET. The almost linearly increasing memory window shown in the inset indicates that ferroelectric polarization in the FeFET is not saturated even at $V_g = \pm 8.0$ V. Reproduced from [15] with permission of IEEE.

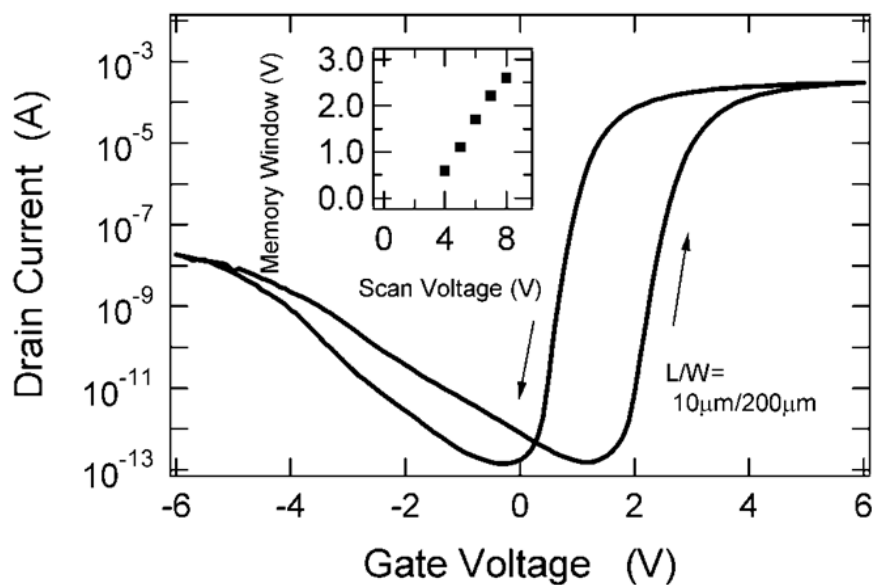
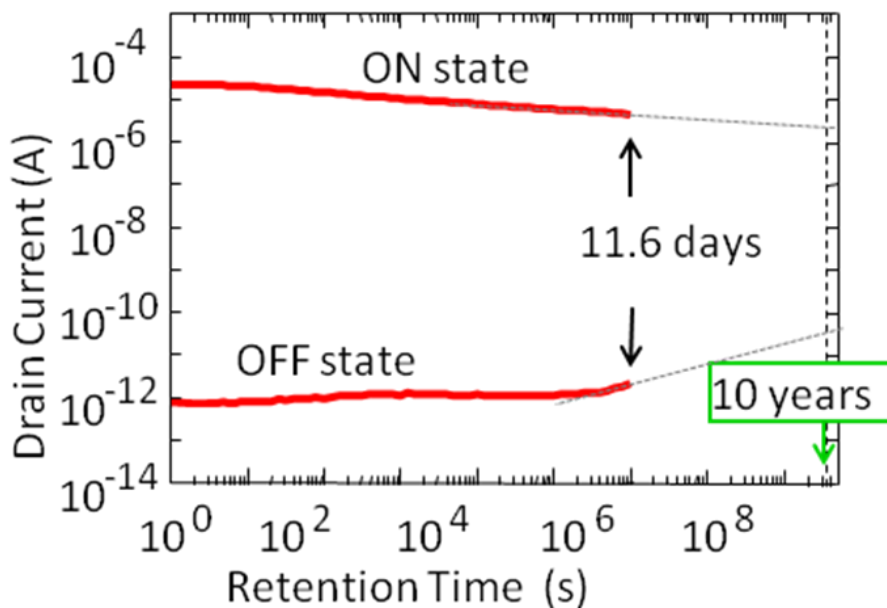
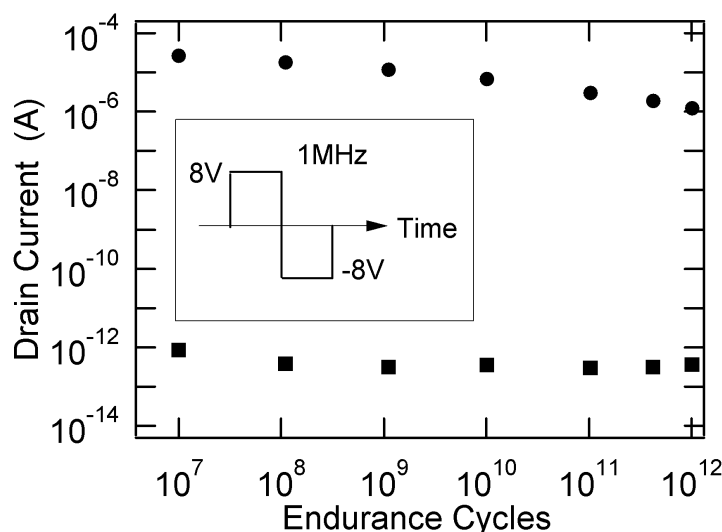


Figure 3. Drain current retention of a Pt/SBT/Hf-Al-O/Si FeFET. Potential 10 year retention is indicated by the extension lines on the measured retention curves. Modified from [15].



Endurance tests were also performed [15]. A cycle of the endurance pulse is shown in the inset of Figure 4. The $I_{d,on}$ and $I_{d,off}$ were measured at $V_{keep} = 2.0$ V after a large number of the endurance pulse cycles were applied to the FET gate electrode. As shown in Figure 4, there was no serious deterioration until 10^{12} cycles. Even after 10^{12} cycles, the $I_{d,on}/I_{d,off}$ ratio was more than 10^6 .

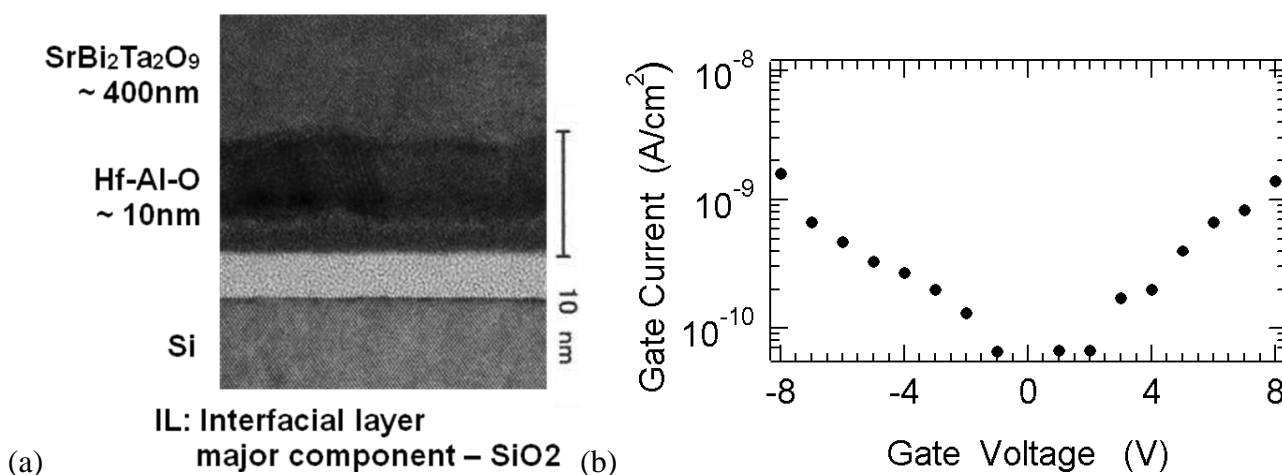
Figure 4. Pulse endurance property of a Pt/SBT/Hf-Al-O/Si FeFET. The inset shows a cycle of the gate voltages which were periodically applied. Reprinted from [15] with permission of IEEE.



The fabrication process is typically as follows: On a substrate with the source- and drain-regions, an Hf-Al-O or HfO₂ buffer insulating layer was deposited in 13 Pa N₂-ambient by a pulsed-laser deposition (PLD) technique. The substrate temperature during the deposition was 200 °C. The SBT

layer was successively deposited by PLD in 13 Pa O₂-ambient at the substrate temperature of 400 °C. The gate metal Pt was electron-beam evaporated. In order to crystallize the SBT layer and to bring out the ferroelectric properties in this layer, the sample was annealed at 800 °C in O₂ for 1 h. Key points for Pt/SBT/Hf-Al-O/Si long-retention FeFETs found in 2002 are summarized as follows: Among MFS, MFIS and MFMIS gate structures, the author chose the MFIS as the most promising structure. As a lower dielectric constant ferroelectric SBT was selected. SBT needs rather high temperature annealing, and in fact a high temperature process of 800 °C and 1h was used to realize the inherent high ferroelectricity of SBT. There are a lot of requirements for the insulating layer (*I*) in MFIS. It should be a good oxygen diffusion barrier to reduce SiO₂-like interfacial layer formation on the Si surface, and should be a high-*k* material to get a large voltage across *F* layer. It should also be strong for SBT annealing around 800 °C and should have chemically stable interface between *F* and *I*. Further, it should have good interface between *I*/Si as the channel of the memory transistors, and should be dense to have small leakage currents. These must have been verified by making MFIS FETs *actually*. The Hf-Al-O chosen as the layer met all the requirements. The interfacial layer was formed but the thickness was acceptable for device operations. (A cross-sectional transmission electron microscopy (TEM) photo is shown in Figure 5(a)) The Hf-Al-O shows dense amorphous properties. The *F*/*I* interface was chemically stable. The gate leakage current was suppressed to the order of or less than 10⁻⁹ A/cm² as shown in Figure 5(b). The composition ratio *x* = 1 of the insulator (HfO₂)_{*x*}(Al₂O₃)_{1-*x*} is HfO₂. Pt/SBT/HfO₂/Si FeFETs have also shown low gate-leakage current and excellent retention characteristics [13,16,27].

Figure 5. (a) Cross-sectional view of a gate by TEM, reprinted from reference [17] with permission of the Japan Society of Applied Physics, and (b) a gate-leakage property of Pt/SBT/Hf-Al-O/Si FeFETs, reprinted from reference [15] with permission of IEEE.



In 2005 we produced self-aligned-gate FeFETs (Figure 6(a)) with gate length $L = 2\mu\text{m}$ and succeeded in measuring 33.5 day-long data retentions (Figure 6(b)) [28]. By extrapolating from the obtained curves for on- and off-retention in Figure 6, I_d on/off ratio over 10⁴ times is expected at 10 years after writing the data. There is also a report of Pt/SBT/HfO₂/Si FeFET with one month retention [29]. Since the FeFET retention was no longer a crucial problem to be solved, we

investigated other reliabilities of device performance at elevated temperatures [30,31], threshold-voltage (V_{th}) distribution [32], and V_{th} adjustment [33].

Figure 6. (a) Self-aligned-gate process for fabricating FeFETs; (b) Drain current retention of a self-aligned-gate Pt/SBT/Hf-Al-O/Si FeFET with $L = 2\mu\text{m}$. Respective curves for on- and off-states were measured over one month. Thicknesses of the SBT and Hf-Al-O were 420 nm and 12 nm. Modified from [28].

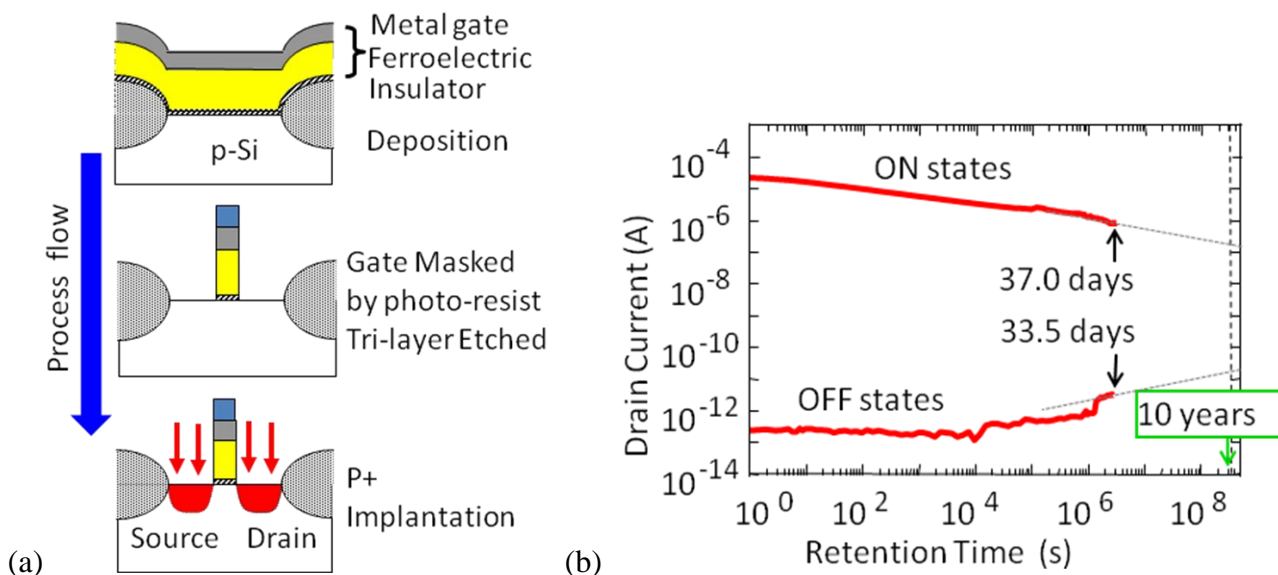


Figure 7. Electrical properties of FeFETs measured at elevated temperatures. (a) Drain current-gate voltage curves, and (b) the drain current retentions of a p -channel Pt/SBT/Hf-Al-O/Si FeFET. Thicknesses of the SBT and Hf-Al-O were 600 nm and 7 nm. Reprinted from [30] with permission of the American Institute of Physics. Good stability of FeFET data retention even at 120 °C was also supported by measuring the retentions of an n -channel Pt/SBT/HfO₂/SiON/Si FeFET (c). Thicknesses of the SBT and HfO₂ were 450 nm and 6 nm. Reprinted from [31] with permission of IOP Publishing Ltd.

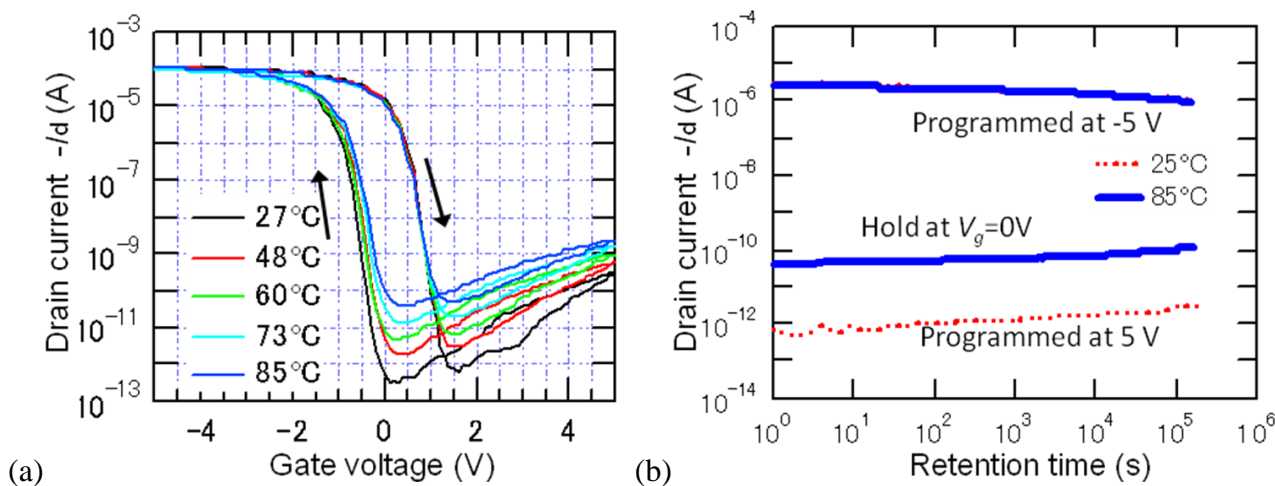
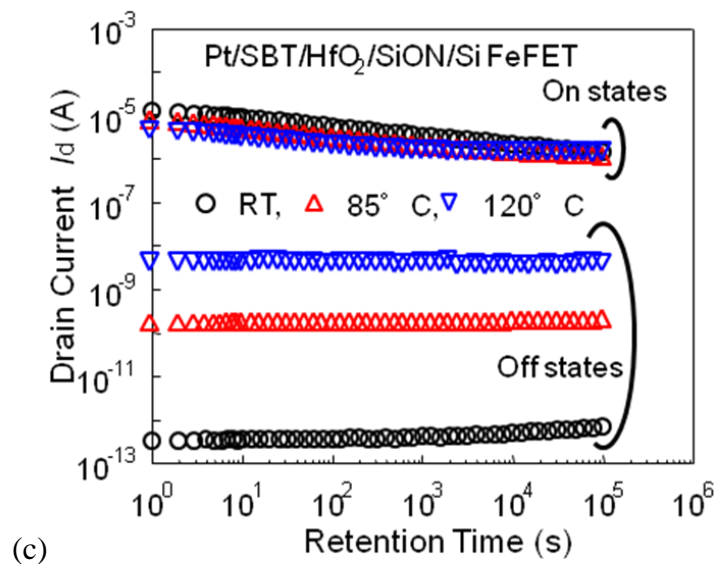


Figure 7. Cont.

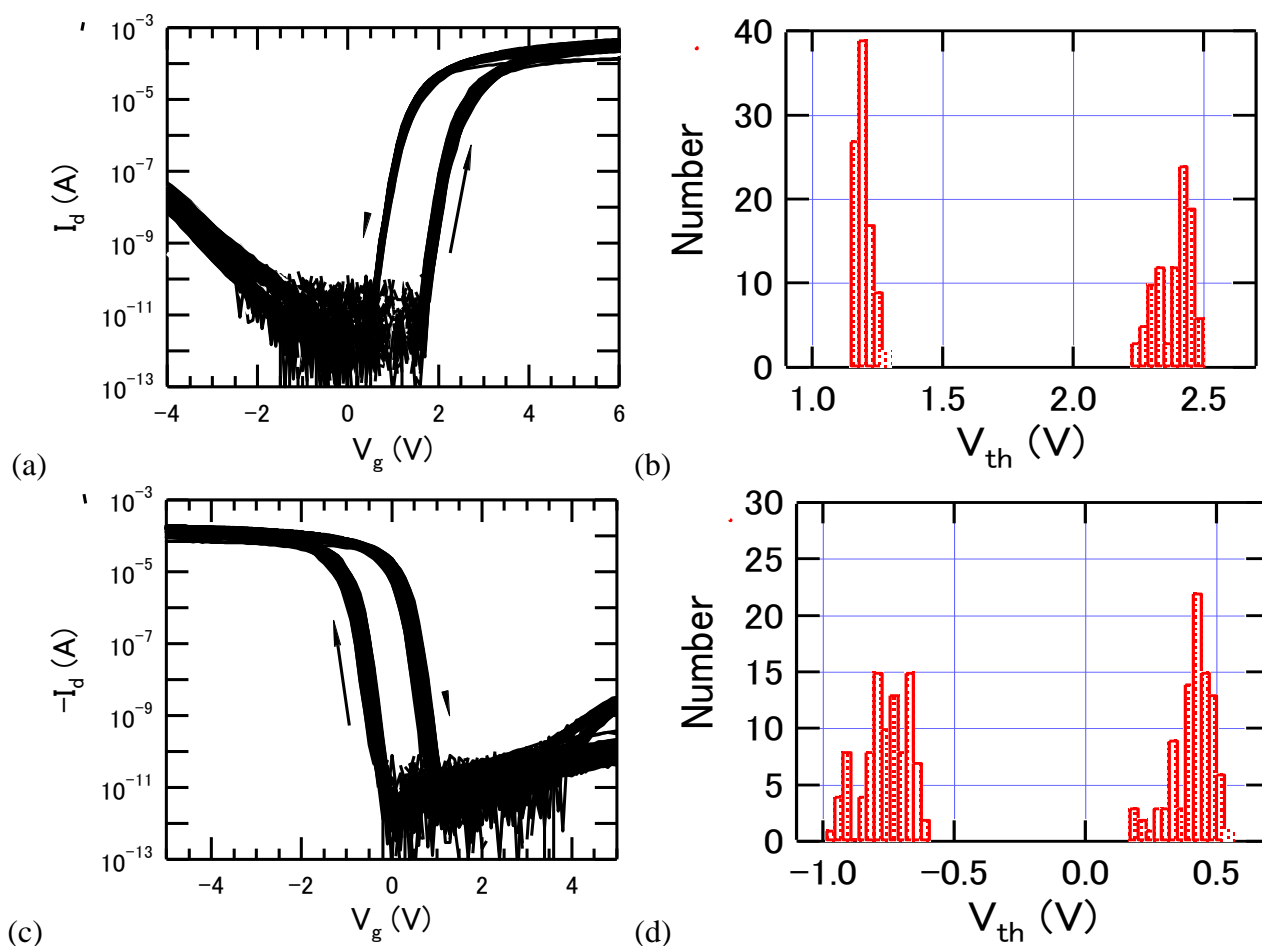


Figures 7 (a) and (b) showed very stable retention performance of a *p*-channel Pt/SBT/Hf-Al-O/Si FeFET at elevated temperatures up to 85 °C [30]. We also succeeded to obtain good retentions of an *n*-channel Pt/SBT/HfO₂/SiON/Si FeFET at 120 °C (Figure 7(c)) [31]. Figure 7(a) indicated that rising current levels of off-state retention curves shown in Figure 7(b) and (c), as the measurement temperature was increased, is due to temperature dependence of source-drain conduction in the FeFETs at their off states.

As shown in Figures 8, statistical distribution of the threshold voltage V_{th} for more than 90 Pt/SBT/Hf-Al-O/Si FeFETs distributed on an area of about $10 \times 11 \text{ mm}^2$ was estimated for both *p*- and *n*-channel devices. The average memory window was nearly 1.2 V at the sweep voltage amplitude of 5 V. The standard deviations of V_{th} were about 7–8% and 3–5% of the memory window for the *n*-channel and *p*-channel FeFETs, respectively. These results indicate that the FeFET technology is up to a promising level for demonstrating an integrated circuit.

With regard to the downsizing of FeFETs, we have very recently fabricated FeFETs with $L = 0.56 \text{ }\mu\text{m}$ by using 200 nm-thick SBT [34]. As well as the early FeFETs introduced above in this chapter, the 0.56 μm FeFET showed good characteristics such as a memory window of 0.93 V, data retention measured over one day, and 10^8 cycle endurance.

Figure 8. (a) Drain current-gate voltage curves of 94 *n*-channel Pt/SBT/Hf-Al-O/Si FeFETs and (b) V_{th} distribution of the 94 *n*-channel FeFETs; (c) Drain current-gate voltage curves of 95 *p*-channel Pt/SBT/Hf-Al-O/Si FeFETs and (d) V_{th} distribution of the 95 *p*-channel FeFETs. Thicknesses of the SBT and Hf-Al-O were 400 nm and 7 nm. Reprinted from reference [32] with permission of IOP Publishing Ltd.



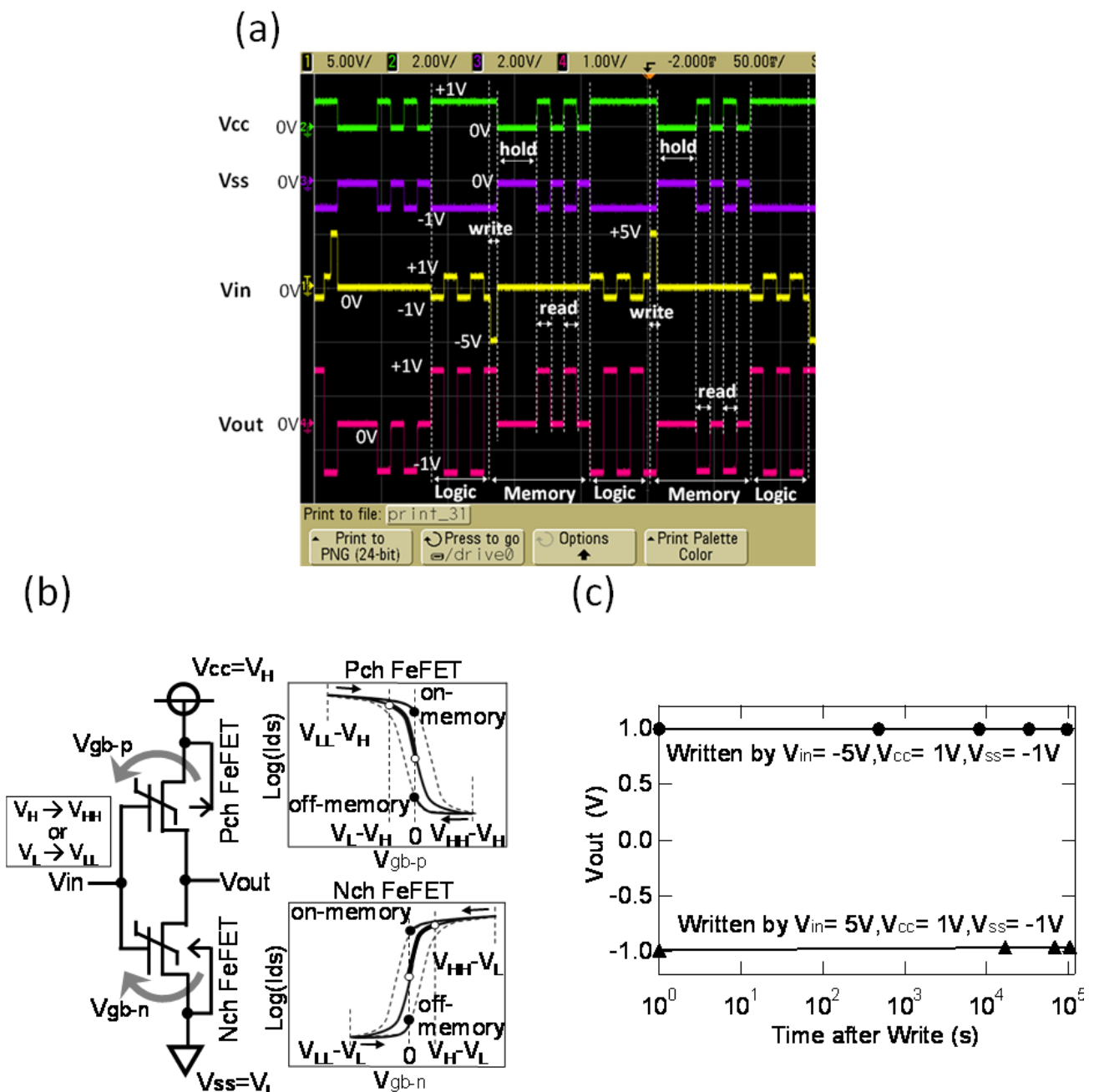
3. FeCMOS Nonvolatile Logic Circuits

Nonvolatile logic circuits with nonvolatile-memory function have attracted much interest for application to next-generation mobile devices with high-speed and low-power consumption [35,36]. We have proposed FeCMOS circuits which are complementary metal-oxide-semiconductor (CMOS) circuits composed of FeFETs instead of conventional MOS FETs [37,38]. The FeFETs have both the *n*-channel-type and *p*-channel-type as conventional MOS FETs have. A FeFET works as a logic transistor or a conventional MOS transistor when a voltage difference between the gate and the substrate (V_{gsub}) is small enough to show negligibly narrow memory windows in I_d - V_g curves. On the other hand, the FeFET works as a nonvolatile memory transistor when the V_{gsub} is large enough to show wide memory windows in the I_d - V_g curves.

Principles of logic-and-memory function switching are demonstrated in Figure 9 which show a single-stage FeFET inverter with the gate-signal amplitude directly changed [37]. At the logic operation, V_{cc} is set to V_H and V_{ss} is set to V_L . V_H or V_L is given to the gate (V_{in}) correspondingly, V_L

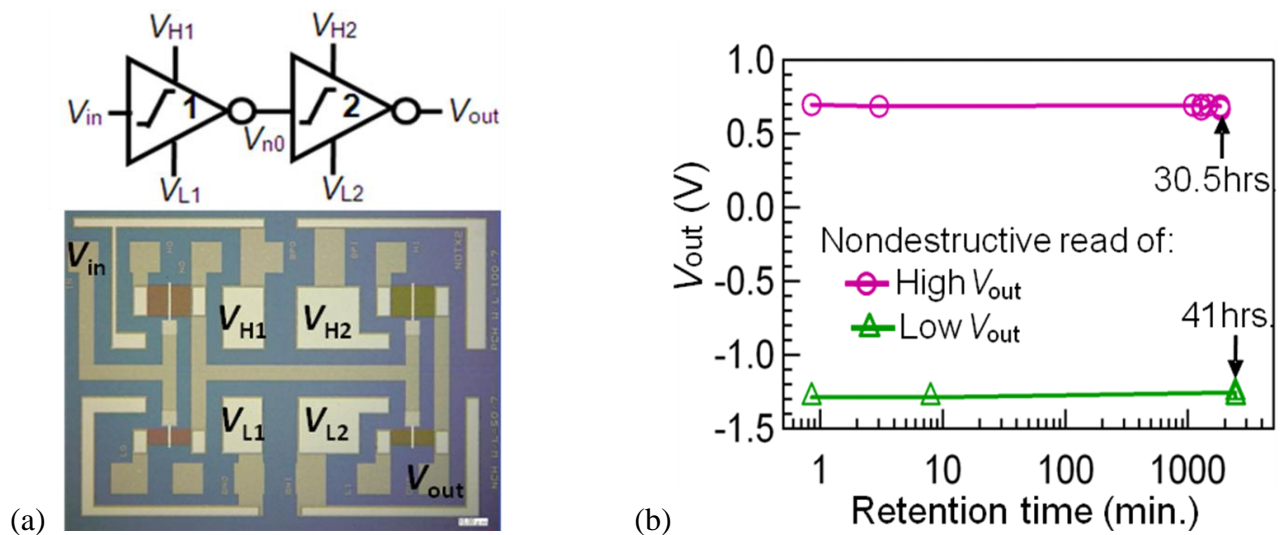
or V_H appear to the output terminal (V_{out}). In this normal inverter operation, the logic swing $V_H - V_L$ is so small that the $I_d - V_g$ curves both for p - and n -channel FeFETs are almost non-hysteretic (Figure 9(a)). At the memory operation, it consists of Write-, Sleep- and Read-modes. In order to write logic data at the input V_{in} , V_{in} is increased to V_{HH} ($V_{HH} \gg V_H$) if $V_{in} = V_H$, and is decreased to V_{LL} ($V_{LL} \ll V_L$) if $V_{in} = V_L$. Then, all supplied voltages are reduced to zero, and the circuit goes into Sleep mode. At the Read, correct information is readout by supplying voltages again to the power supply terminals ($V_{cc} = V_H$ and $V_{ss} = V_L$). This operation is non-destructive as shown in Figure 9(b). The long data retention was confirmed at the measurement of up to 1.2 days (Figure 9(c)).

Figure 9. (a) Schema explaining nonvolatile logic operation of the FeCMOS inverter; (b) Demonstrations of operational switching between logic and memory mode of the FeCMOS inverte; (c) V_{out} -data retention with nondestructive readout. Reproduced from [37] with permission of the Institution of Engineering and Technology.



In a practical usage, we do not know the input V_{in} status, V_H or V_L , at the write timing, but V_{HH} or V_{LL} has to be correctly given. A double-stage FeCMOS inverter circuit (Figure 10(a)) is the simplest circuit for this purpose. For data writing, the supplied voltages of the first stage were enhanced to $V_{H1} = V_H + \delta V_H$ and $V_{L1} = V_L - \delta V_L$. After that, the circuit went in the sleep mode by reducing all supply voltages to zero. Nondestructive data readout was confirmed by supplying again the voltages, V_H and V_L , only to the power supply terminals of the second stage. Data retentions of the circuit logic outputs (V_{out} s) over 30.5 h were measured as shown in Figure 10(b) [38].

Figure 10. (a) Microscopic photo and (b) measured retention with nondestructive readout of double-stage FeCMOS inverter circuit. Reproduced from [38] with permission of IEICE.



4. FeNAND Flash Memory

NAND flash memories are now popular high-density nonvolatile memories [39,40]. Conventional NAND flash memories are constructed by floating-gate (FG) type MOSFET memory cells. The mechanism of program and erase (P/E) operations is electron tunneling through a thin insulator between the FG and semiconductor channel. Program voltage for the FG-NAND cells is around 20 V and P/E cycle endurance is about 10^4 times. As a solution to the problems of high operation voltage and low P/E endurance, we have proposed FeNAND flash memory using FeFETs instead of the FG-MOSFETs as memory cells. The FeNAND will have program voltages around 6 V and more than 10^8 times P/E endurance [41]. The FeNAND is scalable by $4F^2$ rule (F: the feature size) as well as the FG-NAND. Capacitance-coupling noise problem to the adjacent cells can be expected to be small due to the very high permittivity of the ferroelectric even when they are downsized to 10–20 nm in the future. We investigated single-cell performance of the FeNAND. P/E endurance (Figure 11) and data retention after program, erase, V_{pgm} disturb and V_{pass} disturbs (Figure 12) were measured [41]. Ten year-long retention can be expected as suggested in Figure 12.

Figure 11. Program/erase endurance characteristics up to 10^8 cycles of a FeNAND memory cell. Reproduced from [41] with permission of IEEE.

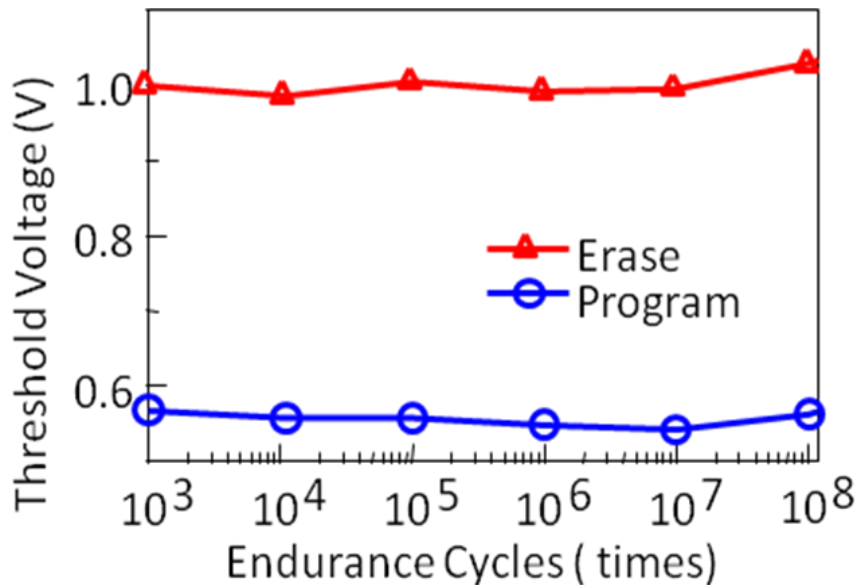


Figure 12. Data retention after the program, erase, V_{pgm} disturb and V_{pass} disturbs. Reproduced from [41] with permission of IEEE.

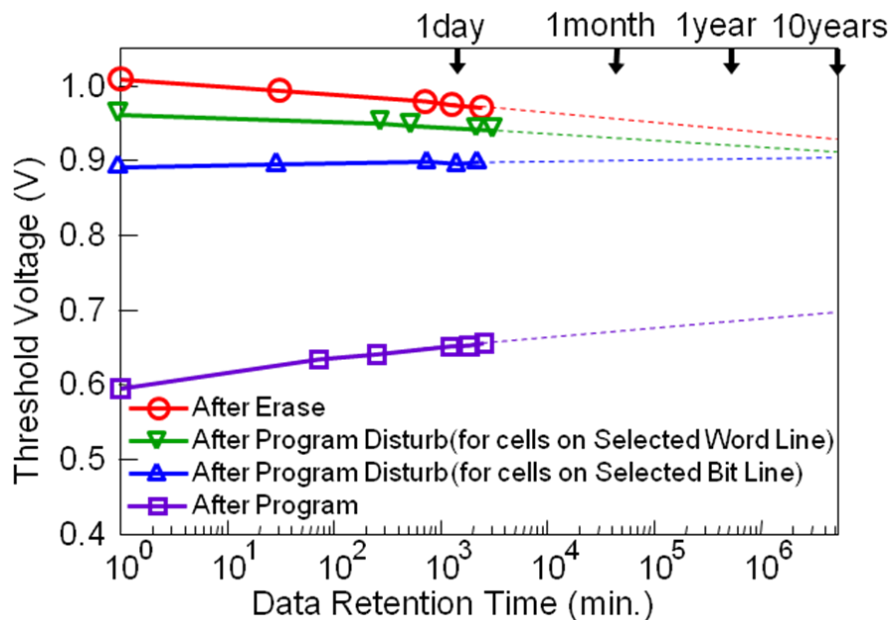
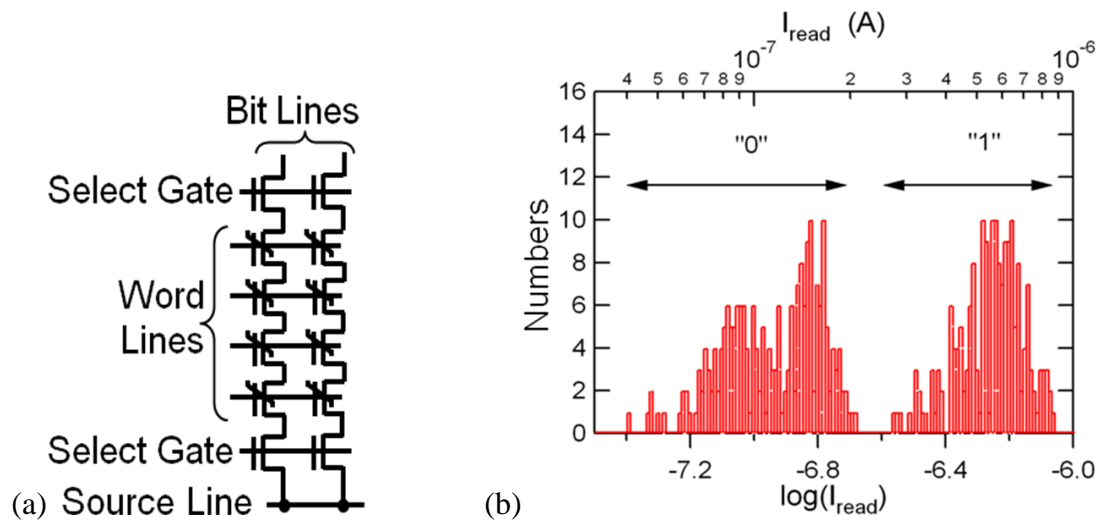


Figure 13. (a) Equivalent circuit of a 4×2 FeNAND memory cell array and (b) distribution of accumulated bit-line currents of 51 programmed patterns, which were measured every time after an erase-and-program cycle. Reproduced from [42] with permission of IOP Publishing Ltd.



Operations of arrayed ferroelectric (Fe-) NAND flash memory cells: erase, program and read, were demonstrated for the first time using a small cell array of four word lines by two NAND strings (Figure 13(a)). The memory cells and select-gate transistors were all *n*-channel Pt/SBT/Hf-Al-O/Si FeFETs. The erase was performed by applying 10 μ s-wide 7 V pulses to *n*- and *p*-wells. The program was performed by applying 10 μ s-wide 7 V pulses to selected word lines. Accumulated read currents of 51 programmed patterns in the FeNAND flash memory cell array successfully showed distribution of the two distinguishable “0” and “1” states [42] (Figure 13(b)). Retention times of bit-line currents were obtained over 33 hours for both the “0” and “1” states in a program pattern.

5. Conclusions

The developed Pt/SBT/Hf-Al-O/Si FeFETs have excellent long retention not only at room temperature but also at the elevated temperature of 120 °C. The FeFET threshold voltage positions could be well controlled and their distributions were small. Nonvolatile logic (FeCMOS) and NAND flash memory (FeNAND) are promising applications, and their fundamental operations were demonstrated by using the FeFET technology that we developed.

Acknowledgements

The author is grateful to the former colleagues R. Ilangoan, Q.-H. Li, S. Wang and T. Horiuchi, and all the current colleagues in our research group. The research project on FeNAND flash memory is running in collaboration with Ken Takeuchi and his group at the University of Tokyo. This work was partially supported by NEDO.

References

1. Tarui, Y.; Hirai, T.; Teramoto, K.; Koike, H.; Nagashima, K. Application of the ferroelectric materials to ULSI memories. *Appl. Surf. Sci.* **1997**, *113*, 656-663.
2. Wu, S.Y. A new ferroelectric memory device, metal-ferroelectric-semiconductor transistor. *IEEE Trans. Electron Devices* **1974**, *ED-21*, 499-504.
3. Sugibuchi, K.; Kurogi, Y.; Endo, N. Ferroelectric field-effect memory device using $\text{Bi}_4\text{Ti}_3\text{O}_{12}$ film. *J. Appl. Phys.* **1975**, *46*, 2877-2881.
4. Higuma, Y.; Matsui, Y.; Okuyama, M.; Nakagawa, T.; Hamakawa, Y. "MFS FET"—A new type of nonvolatile memory switch using PLZT film. *Jpn. J. Appl. Phys.* **1978**, *17*, Suppl. 17, 209-214.
5. Rost, T.A.; Lin, H.; Rabson, T.A. Ferroelectric switching of a field-effect transistor with a lithium niobate gate insulator. *Appl. Phys. Lett.* **1991**, *59*, 3654-3656.
6. Rabson, T.A.; Rost, T.A.; Lin, H. Ferroelectric gate transistors. *Integr. Ferroelectr.* **1995**, *6*, 15-22.
7. Hirai, T.; Fujisaki, Y.; Nagashima, K.; Koike, H.; Tarui, Y. Preparation of $\text{SrBi}_2\text{Ta}_2\text{O}_9$ film at low temperatures and fabrication of a metal/ferroelectric/insulator/semiconductor field effect transistor using $\text{Al/SrBi}_2\text{Ta}_2\text{O}_9/\text{CeO}_2/\text{Si}(100)$ structures. *Jpn. J. Appl. Phys.* **1997**, *36*, 5908-5911.
8. Fujimori, Y.; Izumi, N.; Nakamura, T.; Kamisawa, A. Application of $\text{Sr}_2\text{Nb}_2\text{O}_7$ family ferroelectric films for ferroelectric memory field effect transistor. *Jpn. J. Appl. Phys.* **1998**, *37*, 5207-5210.
9. Tokumitsu, E.; Fujii, G.; Ishiwara, H. Electrical properties of metal-ferroelectric-insulator-semiconductor (MFIS)- and metal-ferroelectric-metal-insulator-semiconductor (MFMIS)-FETs using ferroelectric $\text{SrBi}_2\text{Ta}_2\text{O}_9$ film and $\text{SrTa}_2\text{O}_6/\text{SiON}$ buffer layer. *Jpn. J. Appl. Phys.* **2000**, *39*, 2125-2130.
10. Sugiyama, H.; Kodama, K.; Nakaiso, T.; Noda, M.; Okuyama, M. Electrical properties of metal-ferroelectric-insulator-semiconductor-FET using $\text{SrBi}_2\text{Ta}_2\text{O}_9$ film prepared at low temperature by pulsed laser deposition. *Integr. Ferroelectr.* **2001**, *34*, 1521-1531.
11. Ma, T.P.; Han, J.P. Why is nonvolatile ferroelectric memory field-effect transistor still elusive? *IEEE Electron. Device Lett.* **2002**, *23*, 386-388.
12. Tokumitsu, E.; Okamoto, K.; Ishiwara, H. Low voltage operation of nonvolatile metal-ferroelectric-metal-insulator-semiconductor (MFMIS)-field-effect-transistors (FETs) using $\text{Pt/SrBi}_2\text{Ta}_2\text{O}_9/\text{Pt/SrTa}_2\text{O}_6/\text{SiON/Si}$ structures. *Jpn. J. Appl. Phys.* **2001**, *40*, 2917-2922.
13. Sakai, S. Semiconductor-ferroelectric storage devices and processes for producing the same. U.S. Patent 7,226,795, 2007.
14. Development of the 1T FeRAM: Towards the realization of the ultra-Gbit next-generation semiconductor memory. *AIST Press Release*. Available online: http://www.aist.go.jp/aist_e/latest_research/2002/20021024/20021024.html (accessed on 24 October 2002).
15. Sakai, S.; Ilangoan, R. Metal-ferroelectric-insulator-semiconductor memory FET with long retention and high endurance. *IEEE Electron Device Lett.* **2004**, *25*, 369-371.
16. Sakai, S.; Takahashi, M.; Ilangoan, R. Long-retention ferroelectric-gate FET with a $(\text{HfO}_2)_x(\text{Al}_2\text{O}_3)_{1-x}$ buffer-insulating layer for 1T FeRAM. *Int. Electron Device Meet. Tech. Dig.* **2004**, 915-918.

17. Sakai, S.; Ilangovan, R.; Takahashi, M. Pt/SrBi₂Ta₂O₉/Hf-Al-O/Si field-effect-transistor with long retention using unsaturated ferroelectric polarization switching. *Jpn. J. Appl. Phys.* **2004**, *43*, 7876-7878.
18. Sakai, S. Gate Materials and Fabrication-processes of Metal-ferroelectric-insulator-semiconductor Memory FETs with Long Data Retention. *Adv. Sci. Technol.* **2006**, *45*, 2382-2391.
19. Zhang, F.; Hsu, S.T.; Ono, Y.; Ulrich, B.; Zhang, W.W.; Ying, H.; Stecker, L.; Evans, D.R.; Maa, J. Fabrication and characterization of sub-micron metal-ferroelectric-insulator-semiconductor field effect transistors with Pt/Pb₅Ge₃O₁₁/ZrO₂/Si Structure. *Jpn. J. Appl. Phys.* **2001**, *40*, L635-L637.
20. Li, T.; Hsu, S.T.; Ulrich, B.; Stecker, L.; Evans, D. One transistor ferroelectric memory devices with improved retention characteristics. *Jpn. J. Appl. Phys.* **2002**, *41*, 6890-6894.
21. Su, Y.D.; Shih, W.C.; Lee, J.Y.M. The characterization of retention properties of metal-ferroelectric (PbZr_{0.53}Ti_{0.47}O₃)-insulator (Dy₂O₃, Y₂O₃)-semiconductor devices. *Microelectron. Rel.* **2007**, *47*, 619-622.
22. Cai, D.; Li, P.; Zhang, S.; Zhai, Y.; Ruan, A.; Ou, Y.; Chen, Y.; Wu, D. Fabrication and characteristics of a metal/ferroelectric/polycrystalline silicon/insulator/silicon field effect transistor. *Appl. Phys. Lett.* **2007**, *90*, 153513.
23. Chiang, Y.W.; Wu, J.M. Characterization of metal-ferroelectric (BiFeO₃)-insulator (ZrO₂)-silicon capacitors for nonvolatile memory applications. *Appl. Phys. Lett.* **2007**, *91*, 142103.
24. Shih, W.C.; Juan, P.C.; Lee, J.Y.M. Fabrication and characterization of metal-ferroelectric (PbZr_{0.53}Ti_{0.47}O₃)-Insulator (Y₂O₃)-semiconductor field effect transistors for nonvolatile memory applications. *J. Appl. Phys.* **2008**, *103*, 094110.
25. Lu, X.B.; Maruyama, K.; Ishiwara, H. Metal-ferroelectric-insulator-Si devices using HfTaO buffer layers. *Semicond. Sci. Technol.* **2008**, *23*, 045002.
26. Kim, J.N.; Choi, Y.S.; Park, B.E. (Bi,La)₄Ti₃O₁₂ as a ferroelectric layer and SrTa₂O₆ as a buffer layer for metal-ferroelectric-metal-insulator-semiconductor field-effect transistor. *J. Ceram. Soc. Jpn.* **2009**, *117*, 1032-1034.
27. Aizawa, K.; Park, B.E.; Kawashima, Y.; Takahashi, K.; Ishiwara, H. Impact of HfO₂ buffer layers on data retention characteristics of ferroelectric-gate field-effect transistors. *Appl. Phys. Lett.* **2004**, *85*, 3199-3201.
28. Takahashi, M.; Sakai, S. Self-aligned-gate metal/ferroelectric/insulator/semiconductor field-effect transistors with long memory retention. *Jpn. J. Appl. Phys.* **2005**, *44*, L800-L802.
29. Takahashi, K.; Aizawa, K.; Park, B.E.; Ishiwara, H. Thirty-day-long data retention in ferroelectric-gate field-effect transistors with HfO₂ buffer layers. *Jpn. J. Appl. Phys.* **2005**, *44*, 6218-6220.
30. Li, Q.H.; Sakai, S. Characterization of Pt/SrBi₂Ta₂O₉/Hf-Al-O/Si field-effect transistors at elevated temperatures. *Appl. Phys. Lett.* **2006**, *89*, 222910.
31. Horiuchi, T.; Takahashi, M.; Li, Q.H.; Wang, S.Y.; Sakai, S. Lowered operation voltage in Pt/SBi₂Ta₂O₉/HfO₂/Si ferroelectric-gate field-effect transistors by oxynitriding Si. *Semicond. Sci. Technol.* **2010**, *25*, 055005.
32. Li, Q.H.; Takahashi, M.; Horiuchi, T.; Wang, S.Y.; Sakai, S. Threshold-voltage distribution of Pt/SrBi₂Ta₂O₉/Hf-Al-O/Si MFIS FETs. *Semicond. Sci. Technol.* **2008**, *23*, 045011.

33. Li, Q.H.; Horiuchi, T.; Wang, S.Y.; Takahashi, M.; Sakai, S. Threshold voltage adjustment of ferroelectric-gate field effect transistors by ion implantation. *Semicond. Sci. Technol.* **2009**, *24*, 025012.
34. Le, V.H.; Takahashi, M.; Sakai, S. Fabrication and characterization of sub-0.6- μm ferroelectric-gate field-effect transistors. *Semicond. Sci. Technol.* **2010**, *25*, 115013.
35. Kimura, H.; Hanyu, T.; Kameyama, M.; Fujimori, Y.; Nakamura, T.; Takasu, H. Complementary ferroelectric-capacitor logic for low-power logic-in-memory VLSI. *IEEE J. Solid-State Circuits* **2004**, *39*, 919-926.
36. Matsunaga, S.; Hayakawa, J.; Ikeda, S.; Miura, K.; Hasegawa, H.; Endoh, T.; Ohno, H.; Hanyu, T. Fabrication of a nonvolatile full adder based on logic-in-memory architecture using magnetic tunnel junctions. *Appl. Phys. Express* **2008**, *1*, 091301.
37. Takahashi, M.; Horiuchi, T.; Li, Q.H.; Wang, S.Y.; Sakai, S. Basic operation of novel ferroelectric CMOS circuits. *Electron. Lett.* **2008**, *44*, 467-468.
38. Takahashi, M.; Wang, S.Y.; Horiuchi, T.; Sakai, S. FeCMOS logic inverter circuits with nonvolatile-memory function. *IEICE Electron. Express* **2009**, *6*, 831-836.
39. Takeuchi, K.; Kameda, Y.; Fujimura, S.; Otake, H.; Hosono, K.; Shiga, H.; Watanabe, Y.; Futatsuyama, T.; Shindo, Y.; Kojima, M.; Iwai, M.; Shirakawa, M.; Ichige, M.; Hatakeyama, K.; Tanaka, S.; Kamei, T.; Fu, J.Y.; Cernea, A.; Li, Y.; Higashitani, M.; Hemink, G.; Sato, S.; Oowada, K.; Lee, S.C.; Hayashida, N.; Wan, J.; Lutze, J.; Tsao, S.; Mofidi, M.; Sakurai, K.; Tokiwa, N.; Waki, H.; Nozawa, Y.; Kanazawa, K.; Ohshima, S. A 56nm CMOS 99 mm² 8Gb multi-level NAND flash memory with 10 MB/s program throughput. *IEEE J. Solid-State Circuits* **2006**, 507-516.
40. Takeuchi, K. Novel co-design of NAND flash memory and NAND flash controller circuits sub-30 nm low-power high-speed Solid-State Drives (SSD). In *Proceedings of IEEE Symposium on VLSI Circuits*, Honolulu, HI, USA, 18–20 June 2008; pp. 124-125.
41. Sakai, S.; Takahashi, M.; Takeuchi, K.; Li, Q.H.; Horiuchi, T.; Wang, S.Y.; Yun, K.Y.; Takamiya, M.; Sakurai, T. Highly scalable Fe(ferroelectric)-NAND cell with MFIS (metal-ferroelectric-insulator-semiconductor) structure for sub-10 nm Tera-bit capacity NAND flash memories. In *Proceedings of 23rd IEEE Non-Volatile Semiconductor Memory Workshop/3rd International Conference on Memory Technology and Design*, Opio, France, 18–22 May 2008; pp. 103-105.
42. Wang, S.Y.; Takahashi, M.; Li, Q.H.; Takauchi, K.; Sakai, S. Operational method of a ferroelectric (Fe)-NAND flash memory array. *Semicond. Sci. Technol.* **2009**, *24*, 105029.